Hernández Figueirido, D.; Romero, ML.; Bonet Senach, JL.; Montalva Subirats, JM. (2012). Ultimate capacity of rectangular concrete-filled steel tubular columns under unequal load eccentricities. Journal of Constructional Steel Research. 68(1):107-117. doi:10.1016/j.jcsr.2011.07.014.

Hernández-Figueirido, D., Romero, M.L.*, Bonet, J.L., Montalvá, J.M., Ultimate capacity of rectangular concrete-filled steel tubular columns under unequal load eccentricities, Journal of Constructional Steel Research 2012; 68 (1):107-117.

Ultimate capacity of rectangular concrete-filled steel tubular columns under unequal load eccentricities.

D. Hernández-Figueirido[a], M.L. Romero[b]*, J.L. Bonet[b] and J.M. Montalvá[c]

a Department of Mechanical Engineering and Construction, Universitat Jaume I, Castellón, Spain

b Instituto de Ciencia y Tecnología del Hormigón (ICITECH). Universitat Politècnica de València, Spain

c Dept. Ingeniería de la Construcción, Universitat Politècnica de València, Spain

ABSTRACT

The paper describes 36 experimental tests conducted on rectangular and square tubular columns filled with normal and high strength concrete and subjected to a non-constant bending moment distribution with respect to the weak axis. The test parameters were the nominal strength of concrete (30 and 90 MPa), the cross-section aspect ratio (square or rectangular), the thickness (4 or 5 mm) and the ratio of the top and bottom first order eccentricities e_{top}/e_{bottom} (1, 0.5, 0 and -0.5). The ultimate load of each test was compared with the design loads from Eurocode 4, presenting unsafe results inside a 10% safety margin. The tests show that the use of high strength concrete is more useful for the cases of non-constant bending moment, whereas if the aim is to obtain a more ductile behavior the use of concrete-filled columns is more appealing in the cases of normal strength concrete with non-constant bending moments because, although they resist less axial force than the members with HSC, they obtain a softened post-peak behavior.

Keywords: composite column, concrete-filled tubular columns, high strength concrete, buckling

*Corresponding author: Tel: +34-963877007(ext: 76742) Fax: +34-963879679,

E-mail address: mromero@mes.upv.es

Hernández-Figueirido, D., Romero, M.L.*, Bonet, J.L., Montalvá, J.M., Ultimate capacity of rectangular concrete-filled steel tubular columns under unequal load eccentricities, Journal of Constructional Steel Research 2012; 68 (1):107-117.

NOTATION

e = eccentricity

L = length

b = width of the cross-section

h = height of the cross-section

t = thickness

f_c = cylinder strength of concrete

f_y = yielding stress of steel

HSS= hollow steel sections

CFT =concrete-filled tubular columns

NSC= normal strength concrete

HSC= high strength concrete.

CCR = concrete contribution ratio

SI = strength index

DI = ductility index

Ac = area of concrete

As = area of steel

$(E\cdot I)_{eff}$ = effective flexural stiffness of the composite section.

$\bar{\lambda}$ = relative slenderness $= \sqrt{\dfrac{N_{pl}}{N_{cr}}} = \sqrt{\dfrac{A_c f_c + A_s f_y}{\dfrac{\pi^2 EI_{eff}}{L^2}}}$

N_{exp} = experimental ultimate axial load

$N_{pl,Rd}$ = ultimate load of the composite cross-section following Eurocode 4

$N_{hollow,\,EC3}$ = ultimate load of the hollow steel column following Eurocode 3.

Hernández-Figueirido, D., Romero, M.L.*, Bonet, J.L., Montalvá, J.M., Ultimate capacity of rectangular concrete-filled steel tubular columns under unequal load eccentricities, Journal of Constructional Steel Research 2012; 68 (1):107-117.

1 INTRODUCTION

The use of high strength concrete for CFT columns is becoming popular in multi-story buildings since a substantial reduction of the cross-section is obtained. The composite concrete-steel design methods in the national codes are different for each country (Japan, China, Australia, United States, Europe, etc)[1] and design codes, Eurocode 4 [2] for instance, only allow the use of concrete with a strength lower than 50 MPa (cylinder strength). This means that for high strength concrete the method and the interaction diagrams are not valid. Furthermore, for an equal length of the element, as the cross-section is reduced slenderness is increased and the buckling is more relevant.

The use of normal strength concrete-filled tubular columns has been common for some decades and has been well summarized in a research report by Gourley et al. [3], and more recently, by Zhao et al. [1]. In Europe, the code is based on CIDECT monograph 1 [4] and CIDECT monograph 5 [5].

Recently, much research has appeared on the high performance materials for CFTs, mainly for stub columns or concentric loading, but not focused on overall buckling. The research on high strength concrete (HSC) has shown that the tensile capacity does not increase in the same proportion as the compression capacity. For hollow sections filled with concrete, the tension problem is not as important because the concrete cannot be split off. Therefore, it is this type of section that is most advantageous.

Grauers [6] performed experimental tests on 23 short columns and 23 slender columns, and concluded that although the methods of the different codes were valid, the research should be extended in order to analyze the effect of other parameters. She obtained better ductile behavior introducing a small eccentricity. Later, Bergman [7] studied the confinement mainly for normal strength concrete and partially for high strength concrete, but applying only axial load and not eccentricity. He observed non-ductile behavior once the maximum load was reached.

Rangan and Joyce [8] and Kilpatrick and Rangan [9] presented experimental results from 9 columns for uniaxial bending and 24 columns for double curvature bending, although their tests were limited up to 64 MPa of concrete.

Liu et al. [10] carried out experimental comparisons of the capacity of 22 rectangular sections with the different codes (AISC, ACI, EC4), concluding that Eurocode 4 was not totally safe while other codes over-designed the sections.

Zeghiche and Chaoui [11] stated that the increase of concrete core strength is only effective for shorter columns and decreases with increasing L/D. The D/t ratio, which is one of the parameters that can improve ductile behavior, was not varied in their tests.

Portolés et al. [12] concluded it was clear that the use of HSC in concrete-filled tubular columns does not offer the same improvement as that of NSC in composite behavior. They showed the usefulness of the concrete contribution ratio for different values of slenderness, concrete strength or confinement index for circular CFT columns.

Varma et al. [13] studied the behavior of the square tubular columns asserting that the curvature ductility of high strength square CFT beam-columns (measuring 1.5 meters) decreased significantly with an increase in either the axial load level or the b/t ratio of the steel tube.

Recently some experimental tests have been performed on slender rectangular CFT columns filled with HSC as stated by Lue et al. [15] and Tao et al. [16]. Also Yu et al. [17] published the results of research on circular, square, short, and long CFTs filled with high performance self-consolidating concrete. The results were in agreement using different design codes.

But the cases where the eccentricity is different at both ends of the columns, producing a non-constant bending moment, were not well studied in the bibliography. Besides, if one of the eccentricities is positive and the other negative a double curvature in the element is produced. This problem directly affects slender but not stub columns as it changes the values of the second order bending moments. Eurocode 4 [2] provides an equivalent moment factor β that depends on the type of bending diagram.

Goode [14] compiled the results of several tests, and compared them with Eurocode 4 [2] provisions, reaching the conclusion that although for circular sections it could be extended to 75 MPa, more tests are needed mainly for long circular tubular columns in combination with a bending moment. He did not present any results regarding double curvature.

In fact, there are many papers dealing with this behavior. For circular columns, only Kilpatrick and Rangan [9], and Zeghiche and Chaoui [11] have performed tests with different eccentricities at both ends. In the latter, the test parameters were slenderness, eccentricity, and single and double curvature. The results were compared with EC4 provisions, resulting on the unsafe side for double curvature. They stated that more numerical and experimental tests should be performed to check the validity of the buckling design methods of Eurocode 4 [2] in the case of high strength concrete, for single and double curvature.

The authors compiled and updated the databases of Kim [18] and Goode [14] totaling close to 1400 rectangular experimental tests. From this new database, it was concluded that there is a lack, both for normal and high strength concrete, of tests for columns with non-constant bending moment.

For rectangular columns, Wang [18] presented an experimental study where eight tests on normal strength concrete-filled columns were carried out with end eccentricities which produced moments other than single curvature bending. He concluded that Eurocode 4 was safe but very conservative in some cases.

The authors are performing a research project to study the effect of high strength concrete on the buckling of CFT columns. The project consists of three parts: an experimental study [12], a one-dimensional numerical model [20], and a three-dimensional model. The experimental part of the research project studies circular and rectangular CFT columns for both single and variable curvature.

This paper presents the results of the variable curvature tests program for rectangular columns. It describes tests conducted on rectangular and square tubular columns 2 meters long filled with normal and high strength concrete and subjected to a non-constant bending moment distribution. The test parameters were the nominal strength of concrete (30 and 90 MPa), the type of cross-section (square or rectangular), the thickness (4 or 5 mm), the ratio of the top and bottom first order eccentricities e_{top}/e_{bottom} (1.0, 0.5, 0.0 and -0.5). In these tests the load eccentricity at the ends is fixed and the maximum axial load of the column is evaluated and compared with the design loads from Eurocode 4. Different performance indexes were used to study the effects of the main variables on the load-carrying capacity and ductility.

2 EXPERIMENTAL PROGRAM

In this experimental program thirty-six tests were carried out on normal and high strength concrete columns and six empty hollow steel section columns were also tested, Table 1.

The aim of this was to investigate the effects of the main parameters on their behavior: slenderness of the section (max(b,h)/t), strength of concrete (fc) and single or variable curvature. The buckling lengths of the columns (L) are 2135 mm for all the specimens because although the lengths of the tubes were 2 m, the distance between the hinges needs to add the special assembly length. The nominal cross-section of the tubes (height h × width b x thickness t) were 100 × 100 × 4mm, 100 × 150 × 4mm, 100 × 150 × 5mm, respectively. The thicknesses of the tubes were selected in order to avoid local buckling following Eurocode 4. The nominal cylinder strengths of concrete are 30 or 90 MPa and the axial load is applied with two different eccentricities at the top (20 or 50 mm) with respect to the weak axis of bending to avoid any possible interaction between the strong and weak axes. Different ratios (e_{top}/ e_{bottom}) between the eccentricities are applied in the CFT tests: 1.0, 0.5, 0.0 or -0.5.

Fig. 1 shows the variation of the eccentricities and the first order bending moments. It can be observed that the bending moment of the midspan section varies with r.

All of the tests were performed in the laboratory of the Department of Mechanical Engineering and Construction of the Universitat Jaume I in Castellon, Spain. Six empty tubes were also tested to observe the improvement when the concrete was in-filled (tests 37 to 42).

The nomenclature followed in the tests was:

RXXX.YYY.T_L_CC.SSS_Etop.Ebot (i.e. S100.150.5_2_90.275_20.20), where R stands for rectangular and S for square, XXX is the nominal height in mm, YYY is the nominal width in mm, T is the thickness in mm, L the nominal length in meters, CC the nominal concrete strength in MPa, SSS the nominal yielding steel strength in MPa, Etop is the top eccentricity and Ebot is the bottom eccentricity.

2.1 Material properties

The hollow steel tubes were cold formed and supplied by a manufacturer. The steel grade was S275JR and the real strength (f_y) of the empty tubes was obtained by coupon test and compression stub section, Table 1. The modulus of elasticity Es of the steel was set by European standards with a value of 210 GPa.

All columns were cast using concrete batched in the laboratory with two different nominal concrete strengths of 30 (NSC) and 90 MPa (HSC). The concrete compressive strength f_c was determined from a mean of three 150 × 300 mm cylinders using standard tests. All samples were tested on the same day as the column tests, 28 days, Table 1.

2.2 Fabrication of columns

A 350 mm × 350 mm × 10 mm steel plate was welded to the bottom of each empty steel tube to facilitate the casting of the fresh concrete and to join the element to the pinned support assembly. The elements were then cast in a vertical position and the concrete was vibrated every 0.5m with a needle vibrator. Finally the specimen was covered with wet cloth. Prior to the test, the columns were sealed off with another similar welded plate to ensure perfect contact between the plates and the steel and concrete core.

2.3 Test Setup and procedure

The specimens were tested in a special 5000 kN capacity testing machine in a horizontal position, Fig. 2a. The eccentricity of the compressive load applied was equal at both ends for cases 1 to 12, so the columns were subjected to single curvature bending. It was necessary to build up special assemblies at the pinned ends to apply the load with different eccentricities maintaining the column horizontal for cases 13 to 36, Fig. 2b and d. In particular, the bottom hinge in Fig. 2a could be moved vertically to obtain the necessary eccentricity. Fig. 2a presents a general view of the test for 2 meters long where a special anti-torsion steel frame was built in order to avoid the girder rotation due to the eccentricity of the load in the bottom hinge. Five LVDTs were used to symmetrically measure the deflection of the column at mid length (0.5L) and also at four additional levels (0.25L, 0.37L, 0.625L, 0.75L), Fig. 2c. The strains were measured at the central section using electrical strain gauges which recorded the deformation in two perpendicular directions: longitudinal and transversal, and three locations 0º, 90º, and 180º degrees.

Once the specimen was put in place, it was tested in displacement control in order to measure post-peak behavior.

3 ANALYSIS OF THE RESULTS

3.1. Force-displacement.

Table 1 lists the maximum axial load for the 42 tests. For a better understanding of the behavior Fig. 3 only presents the force-displacement curves for the test with e_{top} = 20mm organized by series. Fig. 3a and Fig. 3b are the cases with a width of 100 mm, but with different variables. In these tests, the general tendency of the curves is as expected: when the eccentricity at the bottom (minimum) is decreased (e_{bottom} = 20, 10, 0, -10 mm), therefore producing variable curvature, Fig. 1, the maximum load is increased because the second order bending moment is reduced.

It is interesting to observe that ductile post-peak behavior is achieved for all the cases, but it is always slightly reduced for cases of HSC in comparison with those of NSC, that is, the slope of the descending branch is more pronounced for the HSC tests. Moreover, the cases of normal strength concrete (NSC) differ from the cases of high strength concrete (HSC) in the descending branch. While the slope is almost the same for the different cases of the eccentricity ratio for NSC, Fig. 3a, for the cases of HSC, Fig. 3b, the slope is more softened for cases with single curvature than for those with variable curvature.

Fig. 3b shows that the case of 100.100.4 filled with HSC with an r = 0.5 seems to fail due to local buckling (by observation), while the other concrete-filled tubes do not present this behavior. It is worth noting that the yielding stress of the steel for this case (fy= 280 MPa) is lower than for the case 100.150.4 with HSC (fy= 424 MPa) where this effect does not appear.

In addition, Fig. 3c to Fig. 3f present the cases with a width of 150 mm. They also exhibit similar behavior to before but bearing a higher axial load, except in the case of 100.150.4 with fc = 30 Mpa and r = -0.5, Fig. 3c, which does not follow the natural trend of the series. In this case the axial load is lower because the yield strength steel of the tube is 20% lower than the other cases (268 MPa), prompting the statement that the failure is very much dependent on the bearing capacity of the hollow steel section.

From all the figures, it can be observed that obviously when the thickness of the tube or the strength of concrete is increased, the load is increased although this latest increment seems to be lower when high strength concrete is introduced. This behavior needs to be studied in greater detail, and introducing a performance index in terms of the strength of concrete (concrete contribution ratio) in the following section.

In Fig. 3e to Fig. 3f it can be observed that for normal and high strength concrete there is no increment in the maximum load between the cases of 100.150.5 with $r = e_{top}/e_{bot} = 0$ and $r = -0.5$.

The same global behavior is observed for the cases where the top eccentricity is 50 mm, not presented in figures to avoid complication, although only two bottom eccentricities were tested ($e_{bottom} = 50, 25$ mm).

However, two graphs of the N_{max} in terms of eccentricity ratio (e_{top}/e_{bot}) summarize all the concrete-filled tests, Fig. 4. From this figure it can be noted that the improvement in the ultimate axial load is higher in the cases of $e_{top} = 20$ than in the cases of $e_{top} = 50$, both for normal and high strength concrete. It is also possible to observe that for the cases of $e_{top} = 50$, there is not a big difference between the cases of $e_{top}/e_{bot} = 1$ and $e_{top}/e_{bot} = 0.5$.

This seems to indicate that the second order effects are very similar in both cases.

Portolés at al [12] stated for circular columns with $e_{top}/e_{bot} = 1$ that for the cases of more slender columns with higher eccentricity, it could be demonstrated that expensive HSC is no more useful than NSC. A more in-depth examination of this statement will be presented in the following sections comparing different cases of e_{top}/e_{bottom}.

Again, if the results of Fig. 3 and Fig. 4 are studied in detail, it can be deduced that for the cases studied reducing the b/t ratio (increasing the thickness t of the cases of 100.150.t) the improvement in force due to the concrete is similar both for normal and high strength concrete, which implies that enhancement is not very dependent on this parameter.

3.2.- Deformed shape.

Fig. 5 presents a comparison of the deformed shape of columns 100.150.5 with different eccentricity ratios ($e_{top}.e_{bottom}$) at the time of failure in each one. The deformed shape is obtained from the 5 LVDTs located in the test.

As can be observed, the displacements are always in the same direction even in the case of double curvature (20-10), and in most of the cases the maximum displacement is achieved in the midspan section, producing a symmetrical deformed shape (20.20, 20.10 or 20.0) both for normal and high strength concrete.

The maximum displacement is located to the left of the midspan section only for the cases of e_{top}/e_{bottom} = -0,5 (i.e 20-10).

For the cases of e_{top} = 50mm the influence of the first order bending moment and second order bending moment is more pronounced and produces the maximum displacement shifts to the left in the case of e_{top}/e_{bottom} = 0,5 (i.e. 50.25).

3.3.- Failure mode.

It was found that the typical failure mode for all the tested specimens was sectional failure and not overall buckling mode. In Fig. 6 the interaction diagrams of two different cases is presented. In these, the axial load versus the total bending moment (Mtotal = N . [e + δ_{LVDT}]) is displayed next to the interaction diagram obtained with Eurocode 4 [1]. For the case of e_{top}/e_{bottom} = 1 (i.e. 20.20) section x/L=0.5 is studied, while for the case of e_{top}/e_{bottom} = -0.5 (i.e. 20.-10) section x/L = 0.375 is studied according to Fig. 5. Sectional failure means that the failure is due to the ultimate state of the materials and not to the geometric nonlinear effect. In the typical overall buckling mode the force-bending moment diagram does not reach the interaction diagram. It can be observed in Fig. 6 that the curves axial load-total bending moment cut the interaction diagrams. The local buckling of the steel tube only occurs in most of the cases in the descending branch and it is not important.

3.4.- Local behavior.

An interesting aspect is the study of the local behavior of rectangular composite sections when subjected to axial load and variable bending moment. As the location of the failure section throughout the length of the column is different for each eccentricity ratio and this was unknown prior to the tests, the strain gauges were placed in the same location for all the cases (x/L = 0.5). The strains in this section depend not only on the axial load but also on the bending moment, which in the midspan section is different for each case of r.

It is worth noting that if the eccentricity ratio is varied (r = 1, 0.5, 0 and -0.5) the first order bending moment, Fig. 1, in the midspan section varies following the next equation:

$$M_{1,midspan} = N. e_{top}. \left[1 - \frac{(1-r)}{2}\right] \quad (1)$$

This thus varies from 1, 0.75, 0.5 or 0.25 times N. e_{top} respectively, so when the eccentricity ratio r decreases, the first order bending moment in the midspan section is reduced, as are the second order bending moments. However, the previous section showed that the maximum axial load increases when r decreases for the ultimate state, making it difficult to infer if in failure the bending moment in the central section will be higher or lower for each case. The strains will also depend on both the axial load and bending moment. So, it is interesting to present a comparison of the measurement from the strain gauges for the different cases of variable bending moment (r = 1, 0.5, 0 and -0.5) in the midspan section. Fig. 7 presents the longitudinal deformation at the left (ε_L) and the transversal deformation at the right (ε_T) of two different points of the section: on the compression side (0º) and on the tension side (180º), Fig. 7e. The strain gauges (ε_{C90} and ε_{T90}) over the symmetry axis (90º) do not provide any valuable information, so they are omitted in the graphs to avoid complication. This figure presents the tests with a 100.100.4 cross-section, fc = 30 MPa and a top eccentricity e_{top} = 20 mm. In addition, Fig. 7a includes two further cases with a top eccentricity e_{top} = 50 mm just to show the variation with respect to e_{top} = 20 mm.

It can be observed that the relationship between the transversal strain at the point of maximum compression ε_{T0} and the longitudinal strain at the same point ε_{L0} is at an almost constant value of -0.3 (the steel Poisson ratio) until the deformation reaches a value close to 1500 -2000 με, which means that there is no composite action up to the yielding of the steel section. This ratio changes after this point but a notable tridimensional behavior only appears in the descending branch, affecting ductility.

It can also be shown that the longitudinal deformation corresponding to the maximum load at the tension point (180º), ε_{L180}, Fig. 7c depends largely on the eccentricity ratio, while the longitudinal deformation corresponding to the maximum load at the compression point (0º), ε_{L0} in Fig. 7a, does not depend on r because these match the deformation of the yielding of the steel which is slightly different for each case, that is, the ε_{L0} of the points of maximum load are very similar if r changes. However ε_{L180} decreases with the eccentricity ratio, achieving negative values (compression) for r = -0.5, meaning that the whole section is under compression. The same behavior is observed in the transversal strains.

When r decreases there is a lower area working under tension and the composite section works better than for equal eccentricities (r = 1). This will mean that the higher strength concretes will present a greater improvement regarding the hollow section if r = -0.5.

An additional commentary can be made on the transversal strains (ε_{T0}, ε_{T90}, and ε_{T180}) because they represented the way that the section changed shape. As was demonstrated by the authors [12], a circular section remains circular if the load is applied concentrically but becomes elliptical or ovoidal if the load is applied with eccentricity. The case of square or rectangular sections is also similar, with the section becoming trapezoidal, as can be seen in the case of transversal strains since these change value and sign, meaning that the final shape of the section will not produce any uniform confinement.

The confinement will be improved only for the cases where all the transversal strains have the same sign (r = 0 or r = -0.5).

4 PERFORMANCE INDEXES

In a previous work [12] the authors demonstrated that for circular slender concrete-filled columns with high eccentricities, an excessive increase in the strength of the concrete is not of great use since no increment in the maximum load was obtained when comparing 70 to 90 MPa. The use of HSC composite columns however was still of interest since they obtain a more ductile behavior. This affirmation was obtained using several performance indexes which will be used again in this paper but applied to rectangular composite sections and with a variable bending moment.

4.1.-Concrete Contribution Ratio (CCR).

As was observed in the previous section, it seems that better use is made of the concrete if the eccentricity ratio decreases, so it is important to establish the importance of the use of high strength concretes compared with that of normal strength concretes. To do so, the concrete contribution ratio (CCR) is defined as the ratio between the maximum load of the composite column and the empty hollow steel member:

$$CCR = \frac{N_{max,exp}}{N_{max,hollow}} \tag{2}$$

This denotes the gain which could be made by using concrete-filled columns rather than bare steel columns. The value of the $N_{max,hollow}$ was obtained from Eurocode 3 [20].

This parameter will be analyzed in terms of the eccentricity ratio r and the steel contribution ratio δ, defined as:

$$\delta = \frac{A_s f_y}{A_c f_c + A_s f_y} \tag{3}$$

Fig. 8a presents the values of the concrete contribution ratio (CCR) in terms of the eccentricity ratio r for the experiments with a section 100.150.5. From this figure, it can be inferred that when HSC is used instead of NSC a better concrete contribution ratio is obtained comparing with single curvature, leading to the conclusion that high strength concrete is used more efficiently if different eccentricities are applied at both ends.

The explanation for this is that when the eccentricity ratio is higher, the concrete has greater importance because a larger portion of the section is compressed, and it is in these cases that high strength concrete is more useful.

In addition Fig. 8b shows the particular cases where the top eccentricity is e_{top} = 20mm and fc = 90 MPa for all the sections (100.100.4, 100.150.4 and 100.150.5). The tests are presented again versus the eccentricity ratio. In this figure it is possible to observe that although the trend is similar for all the types of section, the ones that provide a better CCR are the 100.150.4 series, because these sections have a lower proportion of area of steel compared to the area of concrete.

This statement leads to the introduction of Fig. 8c, where the CCR is presented for all the cases in terms of the steel contribution ratio δ, equation 3. The parameter δ includes not only the influence of fc or fy but also the influence of the thickness t or the influence of the area of steel As. It is clear that when the strength of concrete is increased, the parameter δ is decreased and the CCR is increased. This is not obvious because the authors demonstrated previously [12] that for particular cases of r = 1 if the strength of concrete increases, the CCR keeps constant.

In conclusion, previous statements point to the conclusion that the most influential parameter for incrementing the ultimate axial load is fc, mainly if the eccentricity ratio is lower.

4.2.- Strength Index (SI).

The strength index is defined as:

$$SI = \frac{N_{\max}}{N_{pl,Rd}} = \frac{N_{\max}}{A_c f_c + A_s f_y} \quad (4)$$

It compares the maximum load of the slender column with the resistance of the composite cross-section (without any confinement effect). It denotes the effects of second order effects both due to the length of the column and due to the variable bending moment and is similar to the buckling reduction factor (χ) for a member in axial compression without eccentricity from Eurocode 4, but it cannot be linked to any buckling curves.

Thus, Fig. 9 shows the strength index (SI) in terms of eccentricity ratio for different cases and eccentricities. Fig. 9a displays the SI for the 100.150.5 rectangular columns, where it is possible to observe that the strength index decreases if the strength of concrete increases, meaning that the second order effects are higher for HSC. This is due to the dependence of the second order effects on the relative slenderness λ defined as:

$$\bar{\lambda} = \sqrt{\frac{N_{pl}}{N_{cr}}} = \sqrt{\frac{A_c f_c + A_s f_y}{\frac{\pi^2 EI}{L^2}}} \quad (5)$$

where $EI = E_s I_s + 0.6 E_{cm}.I_c$

and I_s and I_c are the second moment of inertia of the steel tube and the concrete core respectively; E_s is the modulus of elasticity of steel; and E_{cm} is the secant modulus of elasticity of concrete.

The relative slenderness $\bar{\lambda}$ defined in Eurocode 4 is used (instead of L/D) because it includes not only the geometric but also the material properties. It is important to bear in mind that with the same hollow steel section filled with different concretes, the one with higher strength concrete has higher relative slenderness.

It is also important to observe from Fig. 9a that when the eccentricity ratio r is decreased, the SI increases, which means that the second order effects are lower for the case where the bending moment is not constant, just as was expected.

In the same figure it can be noted that the SI is higher for the cases with e = 20 mm than for e = 50 mm. This is because the second order effects are higher for larger eccentricities.

Fig. 9b shows the evolution of SI for the three types of cross-section for the same concrete and eccentricity. In general the three cross-sections have very similar SI values. The low variance may be due to differences in steel and concrete. Nevertheless, what is noticeable is that the strength index (SI) does not appear to be greatly affected by the thickness of the section, since similar results are obtained between 100.150.4 and 100.150.5.

4.3.- Ductility Index (DI).

The ductility of a composite column is one of the most interesting advantages in the comparison of reinforced concrete structures, most especially referring to HSC.

There are several ways to define the ductility index, either using the curvatures or using the displacements. In this paper the second option was selected and defined as the ratio between the displacement corresponding to 85% of the maximum load (in the descending branch) and the displacement from the maximum load:

$$DI = \frac{d(0.85N_{max})}{d(N_{max})} \qquad (6)$$

Fig. 10a shows the ductility index for the rectangular columns 100.150.5 for all the eccentricities and both strengths of concrete. Similar graphs are obtained for the other sections. It is apparent that ductility is reduced by increasing concrete strength but ductile behavior is still achieved. In general, the ductility of rectangular columns is more dependent on the type of concrete than on the eccentricity while for circular columns ductility was important and increased together with eccentricity.

It is important to emphasize the different behaviors of normal strength concrete and high strength concrete cases, Fig. 10a. The ductility of NSC increases if the eccentricity ratio decreases while for HSC the behavior is almost constant. This appears to be due to the brittle behavior of this material which does not benefit from the improvement obtained for NSC.

Fig. 10b displays the DI in terms of the steel reinforcement ratio δ for all the columns. Two different groups of points can be seen in the graph: those on the left correspond to the cases of high strength concrete and those on the right to normal strength concrete, showing that the strength of the concrete is the most important parameter affecting the ductility. Inside each cloud of points the horizontal variation corresponds to a different area of steel while the vertical variation is due to the difference in sections with section 100.100.4 presenting higher ductility and 100.150.4 presenting lower ductility.

These statements lead to the conclusion that if the aim is to obtain a more ductile behavior, the use of concrete-filled columns is more appealing in the cases of normal strength concrete with non-constant bending moments, although these resist less axial force than the members with HSC, they obtain a softened post-peak behavior.

5 COMPARISON WITH EUROCODE 4.

The design of normal strength concrete-filled tubular columns has been common in Europe since the appearance, decades ago, of the first CIDECT [4] monograph, which simplified its applicability for practical engineers. Later research works gave rise to monograph number 5, CIDECT [5]. All these documents were the basis of the first version of Eurocode 4 [2] which pays special attention to concrete-filled columns. It limits the cylinder strength of concrete to 50 MPa.

The experiments in this study aim to clarify whether Eurocode 4 is still applicable to 90 Mpa and also if the factor β that takes into account the influence of a non-constant bending moment is correct or not. Furthermore, since these tests are rectangular, the increment in the resistance of the cross-section due to the confinement effect is ignored. In addition the partial safety factor for steel and concrete are fixed to 1, and the empty tubes are not included in the method because these have to be calculated using Eurocode 3.

Table 1 presents a comparison between the experiments (N_{exp}) and the design load of Eurocode 4 (N_{EC4}).

To calculate the load N_{EC4}, clause 6.7.3.4.5 of Eurocode 4 [1] is used. It affirms that within the column length, second order effects may be allowed for by multiplying the greatest first order design bending moment M_{Ed} by a factor k given by:

$$k = \frac{\beta}{1 - \frac{N_{Ed}}{N_{cr,eff}}} \tag{7}$$

where:

$N_{cr,eff}$ is the critical axial force ($\pi^2 EI_{eff}/L^2$) for the relevant axis and corresponds to the effective flexural stiffness, with the effective length taken as the column length, and β is an equivalent moment factor equal to:

$$\beta = 0{,}66 + 0{,}44r \quad \text{but } \beta \geq 0{,}44 \tag{8}$$

where M_{ed} and rM_{Ed} are the end moments from first order or second order global analysis, Fig. 11.

From Table 1 it can be stated that most of the cases are on the unsafe side (Nexp/Nec4 < 1) both for variable curvature and single curvature; although they are inside the safety margin of 10% since a mean value of 0.91 and a standard deviation of 0.07 were obtained. But the cases of 50.25 and 20-10 present a higher difference. Fig. 12 shows a comparison between the maximum loads obtained in the experiments N_{max} and those obtained from Eurocode 4, N_{EC4}, showing most of them below the bisector. Some of the cases are even below the 10% of safety margin, which means that the Eurocode is unsafe for those cases.

From a detailed study of Table 1 it can be inferred that Eurocode 4 is unsafe for two different groups of cases: first for normal strength concrete and eccentricity ratio e_{top}/e_{bottom} equal to 1 or 0.5, and the second in contrast for HSC for cases with r = -0.5.

The first group corresponds to the cases where there are more second order effects and the concrete contributes less and the second ones to those where there are lower second order effects but the concrete is higher strength.

The first group indicates that the equation of the stiffness of the section E.I needs correction, and the second one indicates that the factor β or r must somehow be included in the confinement effect.

Accordingly, the authors consider that it is necessary to provide more data to achieve reliable results. To do so a numerical model for the accurate prediction of high strength concrete composite columns is needed.

6 CONCLUSIONS

The paper is focused on the presentation of 36 experimental tests of concrete-filled tubular columns subjected to axial load and single or variable curvature.

The following conclusions can be summarized:

- For the cases studied reducing the b/t ratio (increasing the thickness t of the cases of 100.150.t) the improvement in force due to the concrete is similar both for normal and high strength concrete, implying that enhancement is not very dependent on this parameter.
- When the eccentricity ratio r decreases there is a lower area working under tension and the composite section works better than for equal eccentricities (r = 1). This entails the higher strength concrete presenting improvement compared to the hollow section if r = -0.5.

- Confinement will be improved only for the cases where all the transversal strains have the same sign ($r = 0$ or $r = -0.5$).
- For the limited tests of this experimental campaign the most influential parameter in incrementing the ultimate axial load is the strength of concrete mainly if the eccentricity ratio is lower. It is worth noting that in this paper the difference of concrete strength is very huge (30 MPa and 90 MPa) while the difference of tube thickness is small (4mm and 5mm), so the concrete strength dominates the behavior of the specimens including ultimate strength and ductility. However, if the concrete strength were 30 and 60 MPa and the tube thickness are 4mm and 10mm, maybe the steel tube thickness dominates the behavior of the specimens and the conclusion maybe cannot be drawn.
- The strength index (SI) does not seem to be greatly affected by the thickness of the section, since similar results are obtained between the different thicknesses.
- The ductility of rectangular columns is more dependent on the type of concrete than on the eccentricity. The ductility of NSC increases if the eccentricity ratio decreases while for HSC the behavior is almost constant. This means that the strength of the concrete is again the most predominant parameter affecting ductility.
- If the aim is to obtain a more ductile behavior, the use of concrete-filled columns is more appealing in cases of normal strength concrete with non-constant bending moments because although they resist less axial force than the members with HSC, they obtain a softened post-peak behavior.

The experimental ultimate load of each test was compared with the design loads from Eurocode 4, where most of the cases are on the unsafe side ($N_{EXP}/N_{EC4} < 1$) both for variable curvature and single curvature, although this is inside the safety margin of 10%.

Hernández-Figueirido, D., Romero, M.L.*, Bonet, J.L., Montalvá, J.M., Ultimate capacity of rectangular concrete-filled steel tubular columns under unequal load eccentricities, Journal of Constructional Steel Research 2012; 68 (1):107-117.

The authors will perform further work to provide more data to achieve reliable results, using numerical models in order to improve the equation of the stiffness of the section E.I, the equivalent moment factor β and study the effect of the eccentricity ratio in the confinement effect.

ACKNOWLEDGEMENTS

The authors wish to express their sincere gratitude to the Spanish Ministry of Education for help provided through project BIA2005_255 and BIA2009_9411, and to the European Community for FEDER funds.

REFERENCES

[1] Zhao XL, Han LH, Lu H. Concrete-filled tubular members. 1st Ed. Oxon: Spon Press; 2010.

[2] European Committee of Standardization. EN 1994-1-1:2004 Eurocode 4: Design of composite steel and concrete structures Part 1-1: General rules and rules for buildings. 2004.

[3] Gourley, B. C., Tort, C., Denavit, M. D., Schiller, P. H., and Hajjar, J. F. "A Synopsis of Studies of the Monotonic and Cyclic Behavior of Concrete-Filled Steel Tube Beam-Columns", Report No. UILU-ENG-2008-1802, Newmark Structural Laboratory Report Series (ISSN 1940-9826), Department of Civil and Environmental Engineering, University of Illinois at Urbana-Champaign, Urbana, Illinois.USA, 2008.

[4] CIDECT." Monograph nº 1: Concrete filled hollow section steel columns design manual". British edition, 1970.

[5] CIDECT. "Monograph nº 5: Calcules Poteaux en Profils Creux remplis de Béton", 1979.

[6] Grauers, M. "Composite columns of hollow sections filled with high strength concrete". Research report. Chalmers University of Technology, Goteborg, 1993.

Hernández-Figueirido, D., Romero, M.L.*, Bonet, J.L., Montalvá, J.M., Ultimate capacity of rectangular concrete-filled steel tubular columns under unequal load eccentricities, Journal of Constructional Steel Research 2012; 68 (1):107-117.

[7] Bergmann, R. “Load introduction in composite columns filled with High strength concrete”, Proceedings of the 6th International Symposium on Tubular Structures, Monash University, Melbourne, Australia, 1994.

[8] Rangan B. & Joyce M. “Strength Of Eccentrically Loaded Slender Steel Tubular Columns Filled With High-Strength Concrete”, ACI Structural journal, 89 (6): 676-681, 1992.

[9] Kilpatrick A.E. & Rangan B.V. “Tests on High-Strength Concrete-Filled Steel Tubular Columns”. ACI Structural journal, 96 (2): 268-275, 1999.

[10] Liu DL, Gho WM & Yuan H. “Ultimate capacity of high-strength rectangular concrete-filled steel hollow section stub columns”, Journal of constructional steel research, 59 (12): 1499-1515, 2003.

[11] Zeghiche J, Chaoui K. An experimental behaviour of concrete-filled steel tubular columns. J Construct Steel Res 2005; 61(1): 53-66.

[12] Portolés J.M., Romero M.L., Bonet J.L. and Filippou F.C., Experimental study of high strength concrete-filled circular tubular columns under eccentric loading, Journal of Constructional Steel Research 2010; 67:623-633.

[13] Varma A.H., Ricles J.M., Sause R., et al. “Experimental behavior of high strength square concrete-filled steel tube beam-columns”, Journal of Structural Engineering-ASCE, 128 (3): 309-318, 2002.

[14] Goode, CD. “Composite columns-1819 tests on concrete filled tube columns compared with Eurocode 4”, The Structural Engineer, 86(16): 33-38, 2008.

[15] Lue D, Liu J, Yen T.. Experimental study on rectangular CFT columns with high-strength concrete. Journal of constructional steel research 2007; 63(1):37-44.

[16] Tao Z, Han L, Wang D. Experimental behaviour of concrete-filled stiffened thin-walled steel tubular columns. Thin-walled structures 2007; 45(5):517-527.

[17] Yu Q, Tao Z, Wu Y. Experimental behaviour of high performance concrete-filled steel tubular columns. Thin-walled structures 2007; 46(4):362-370.

[18] Kim DK. A database for composite columns. Ms Thesis. Georgia Tech University. U.S.A. 2005.

[19] Wang YC. Tests on slender composite columns. Journal of constructional steel research 1999; 49(1):25-41.

[20] European Committee of Standardization. EN 1993-1-1:2005 Eurocode 3: Design of steel structures Part 1-1: General rules and rules for buildings. 2005.

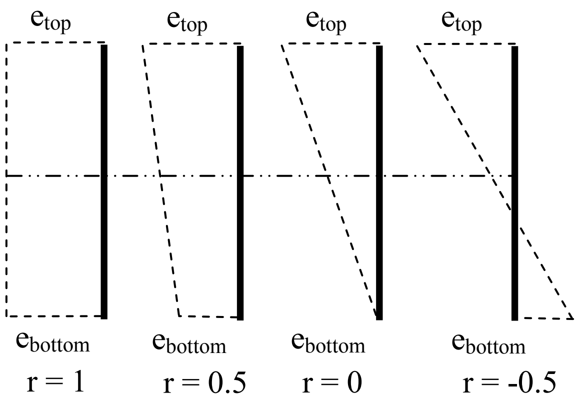

Fig. 1. Variation of the eccentricities and first order bending moment.

Hernández-Figueirido, D., Romero, M.L.*, Bonet, J.L., Montalvá, J.M., Ultimate capacity of rectangular concrete-filled steel tubular columns under unequal load eccentricities, Journal of Constructional Steel Research 2012; 68 (1):107-117.

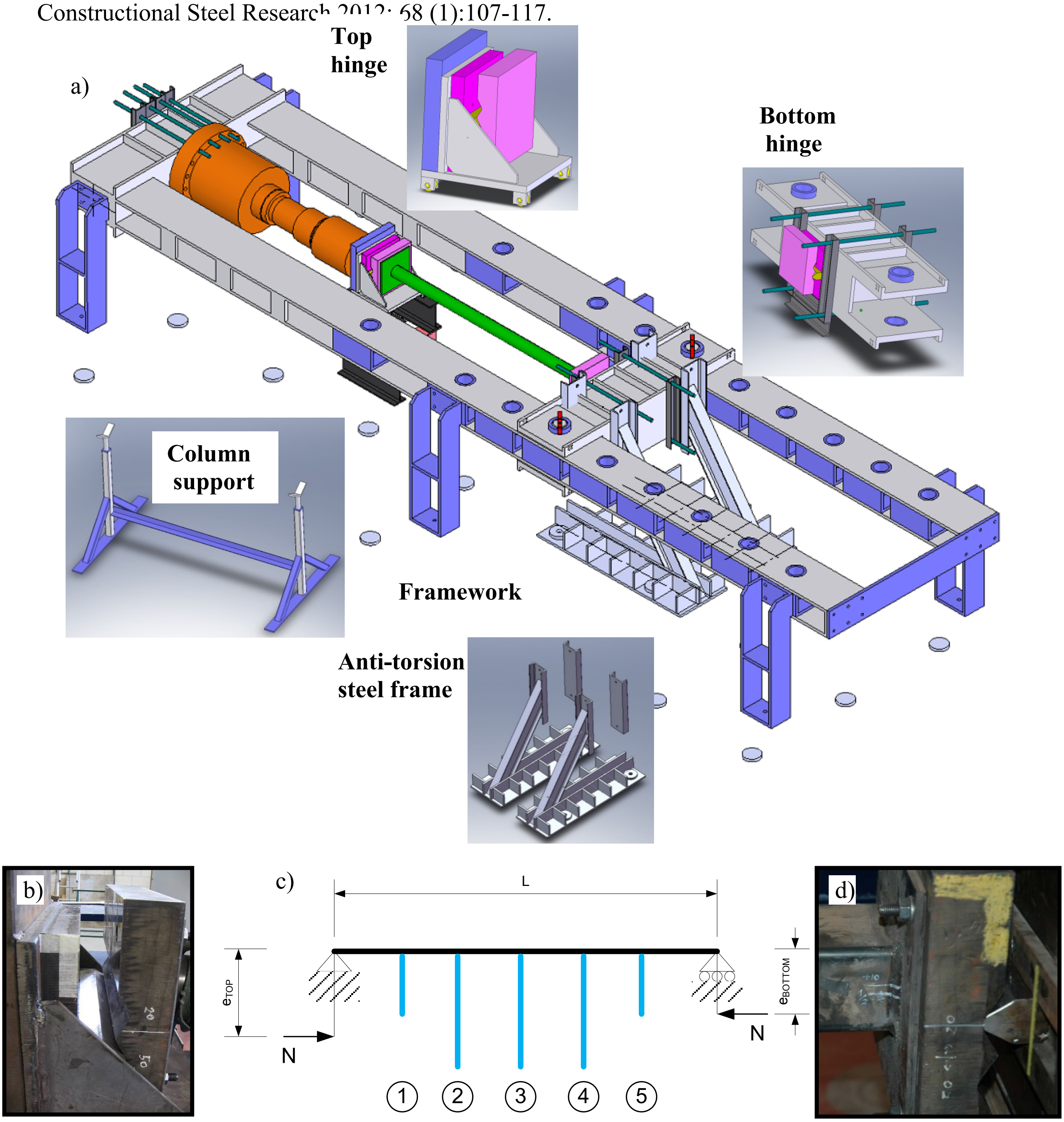

Fig. 2. General view and details of the tests.

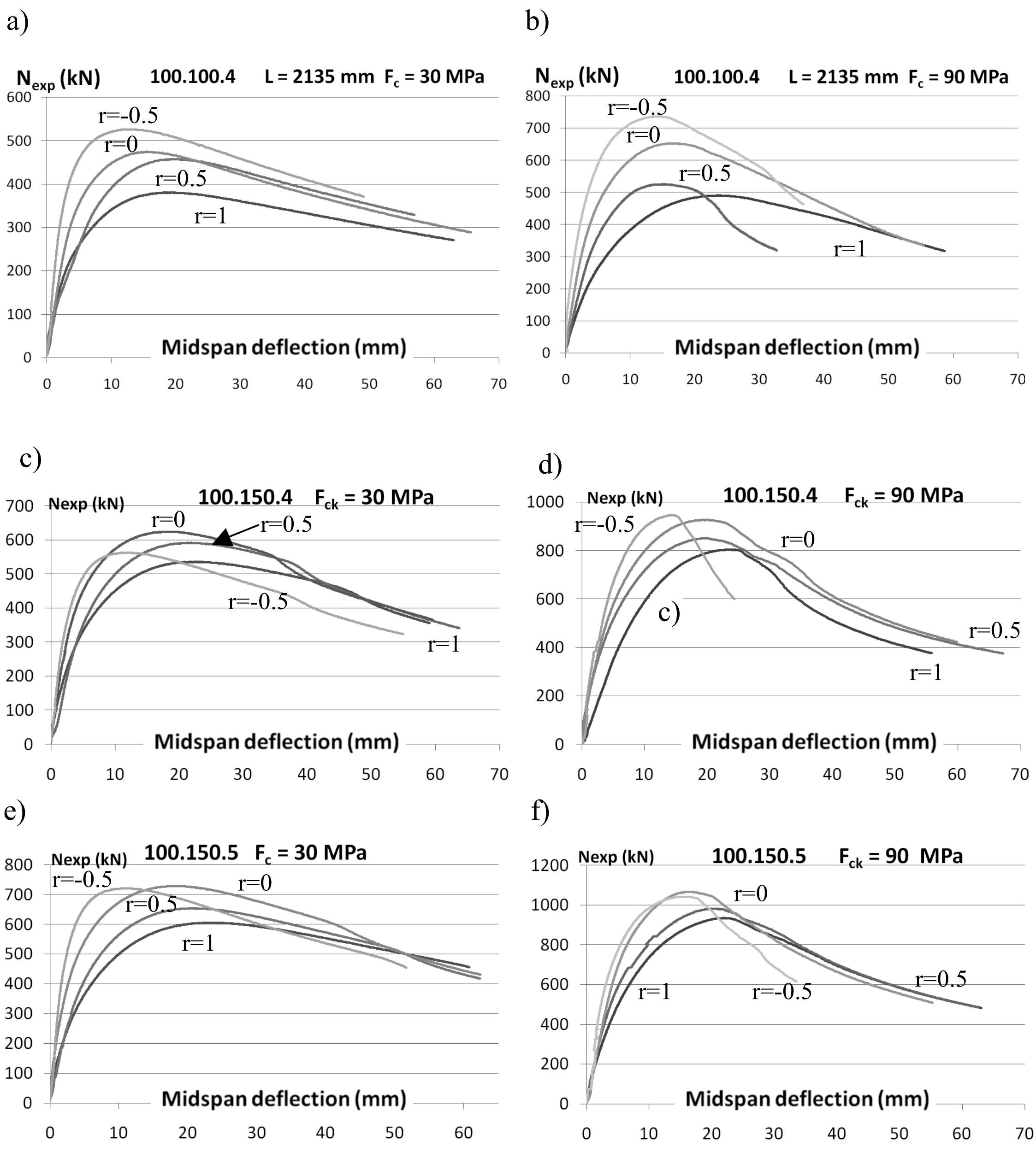

Fig. 3. Axial load versus midspan displacement series

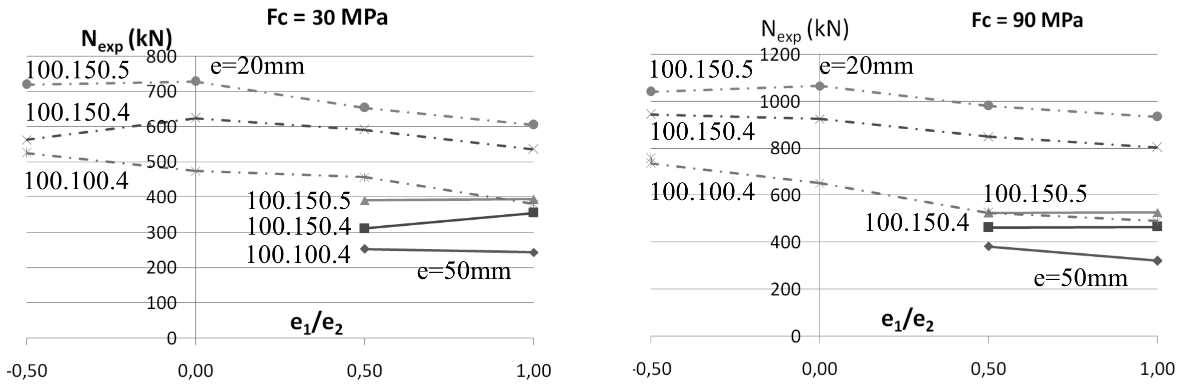

a) b)

Fig. 4. Axial load versus eccentricity ratio

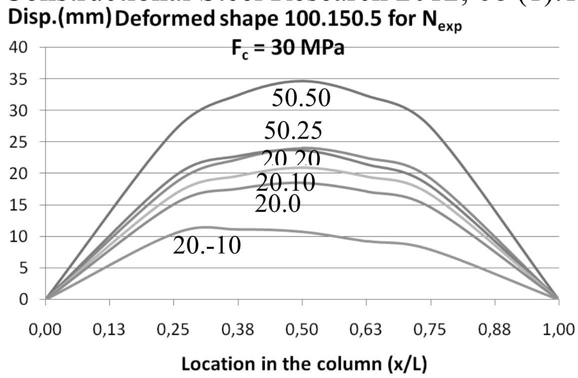

a)

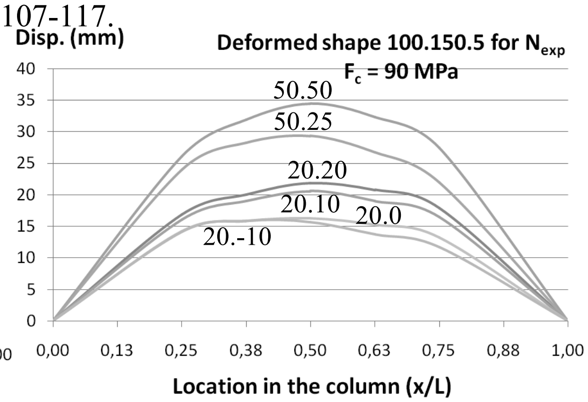

b)

Fig. 5. Deformed shape for Nmax for 100.150.5 and NSC

Hernández-Figueirido, D., Romero, M.L.*, Bonet, J.L., Montalvá, J.M., Ultimate capacity of rectangular concrete-filled steel tubular columns under unequal load eccentricities, Journal of Constructional Steel Research 2012; 68 (1):107-117.

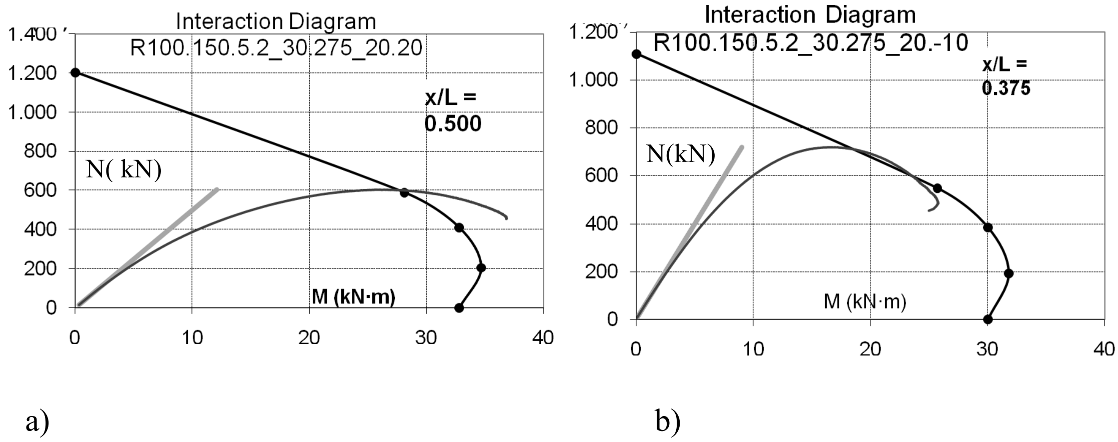

Fig. 6. Interaction diagrams of 100.150.5, fc = 30 and e_{top} = 20mm. a) r = 1 b) r = -0.5

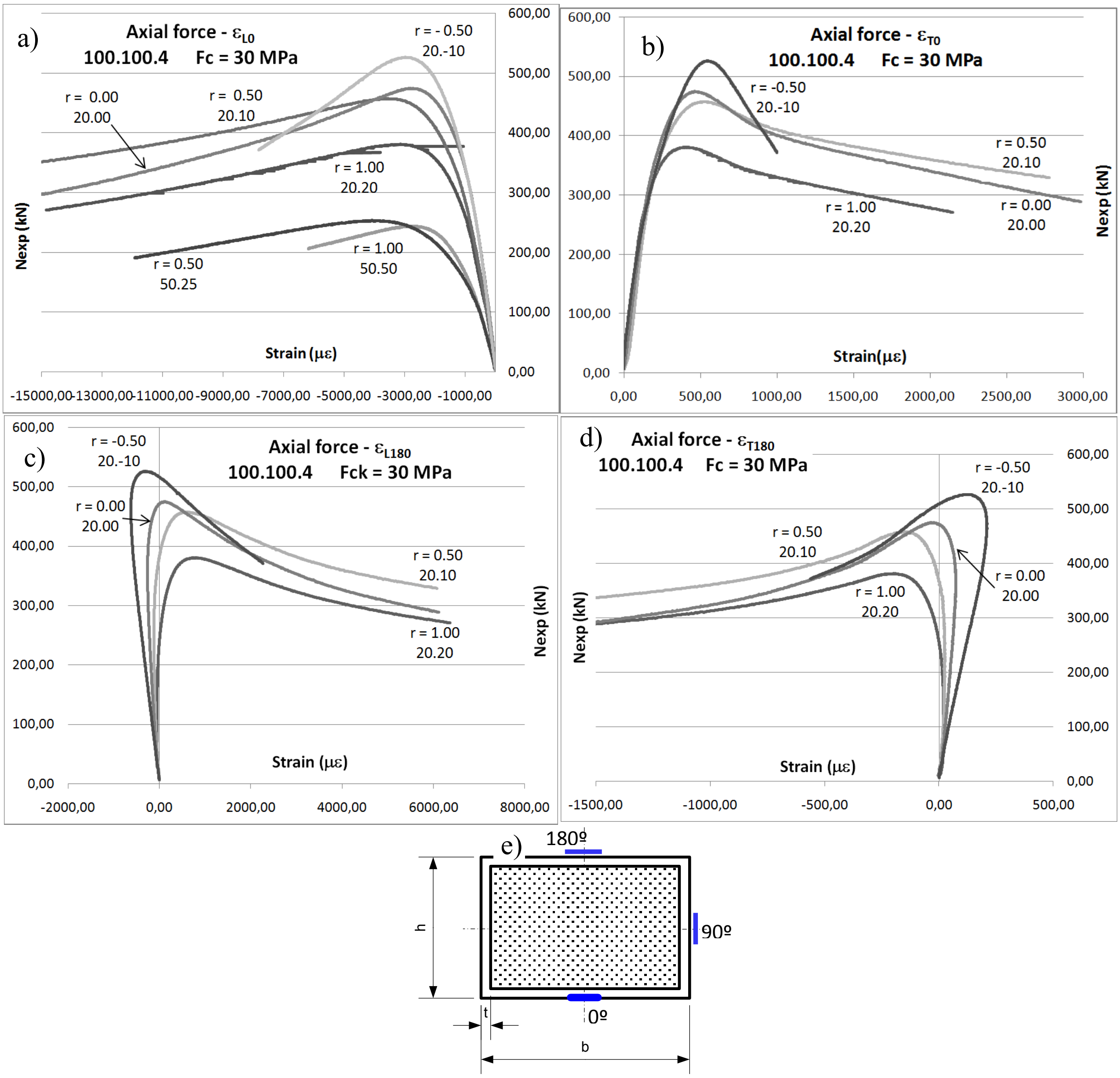

Fig. 7. Longitudinal (ε_L) and transversal strains (ε_T) at 0º and 180º

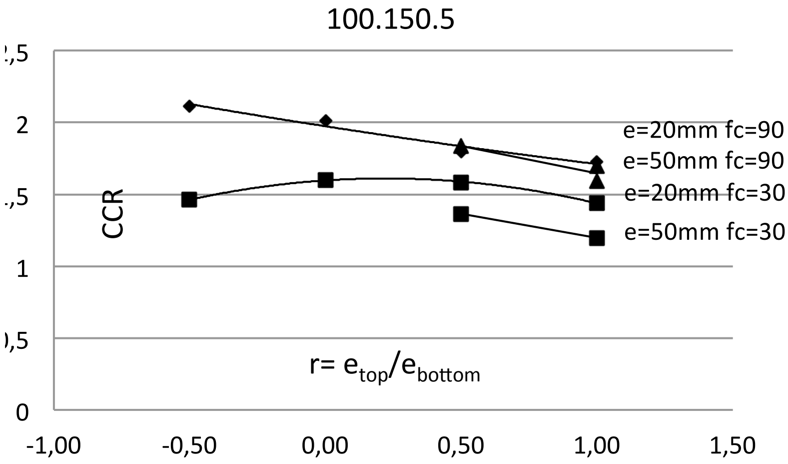

a)

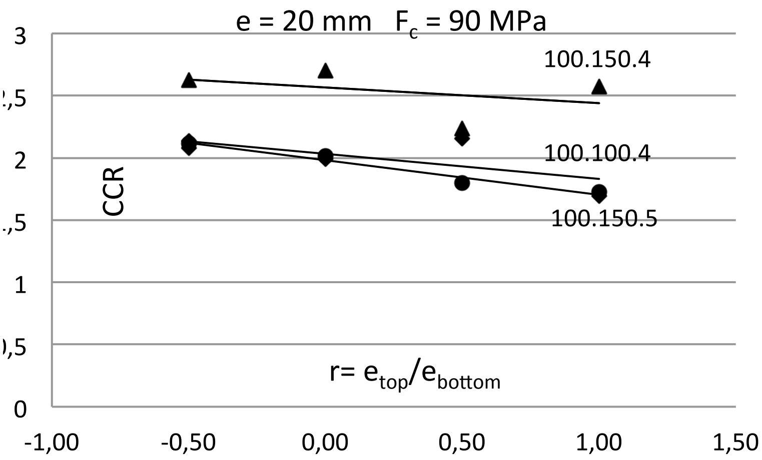

b)

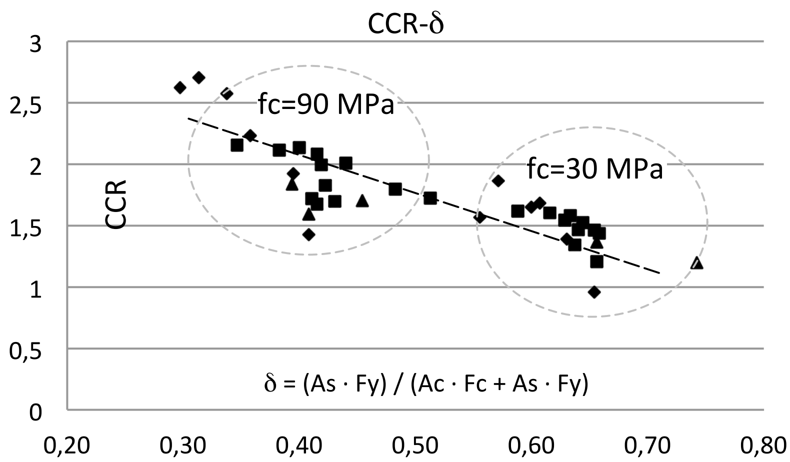

Fig. 8. Concrete contribution ratio.

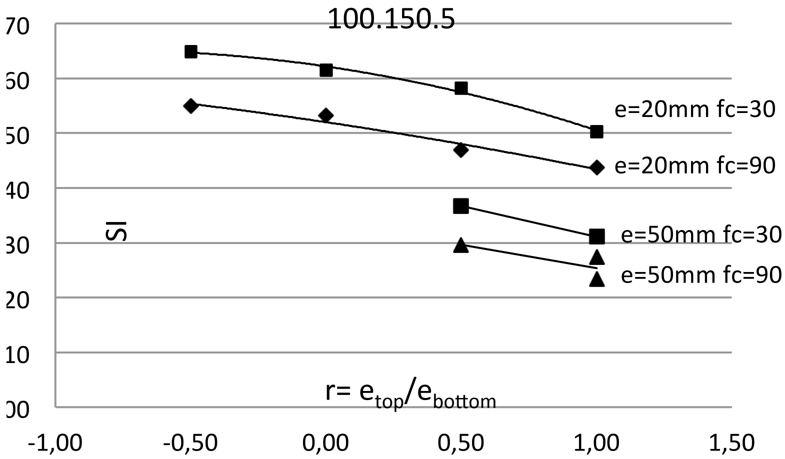

(a)

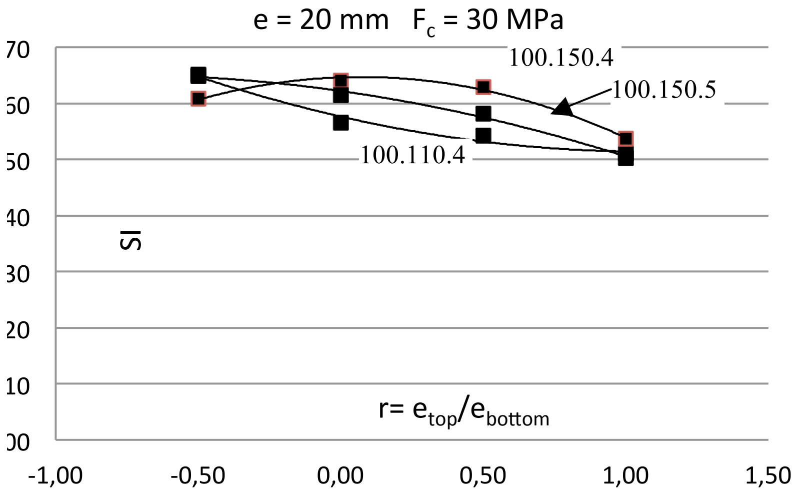

(b)

Fig. 9. Strength Index (SI)

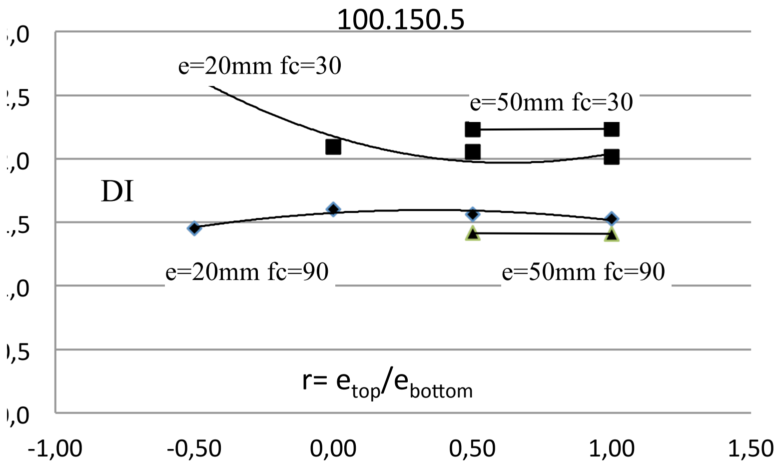

(a)

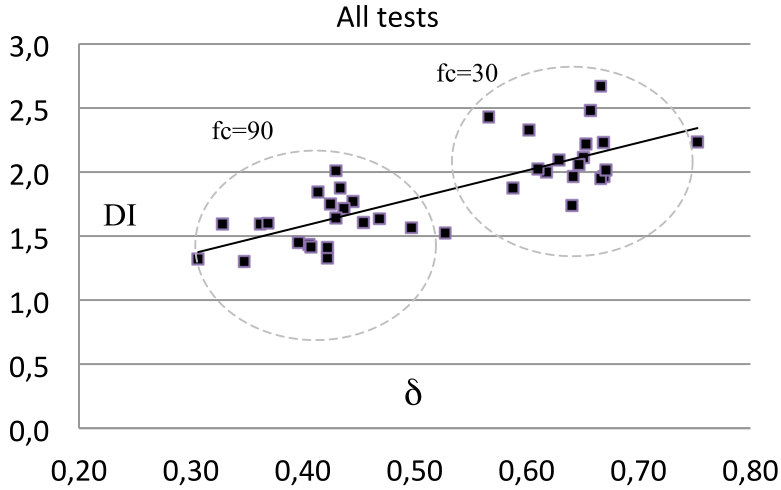

Fig. 10. Ductility Index (DI)

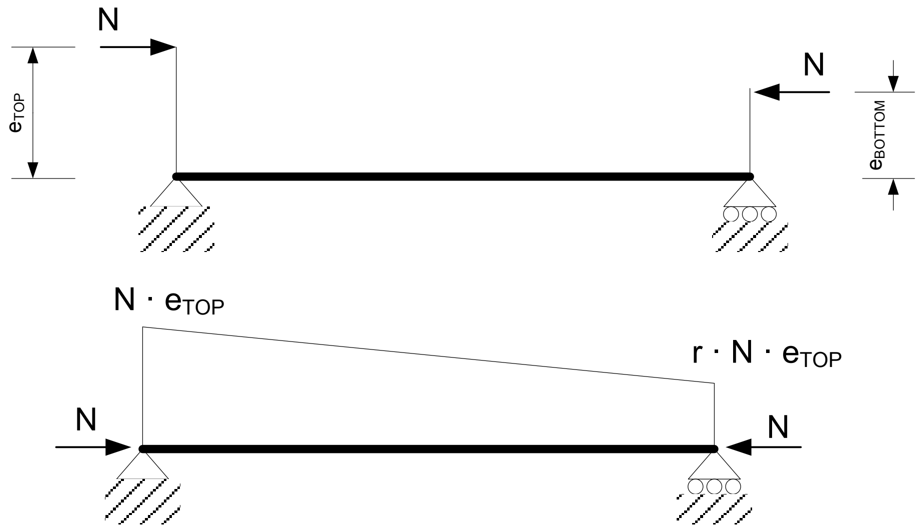

Fig. 11. Non-constant bending moment from Eurocode 4 [2]

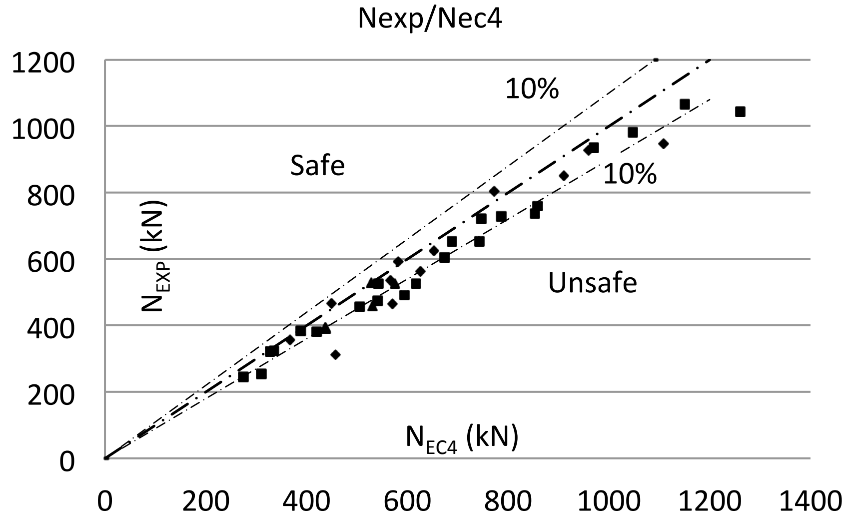

Fig. 12. Error between experimental ultimate load and Eurocode 4 provisions

Hernández-Figueirido, D., Romero, M.L.*, Bonet, J.L., Montalvá, J.M., Ultimate capacity of rectangular concrete-filled steel tubular columns under unequal load eccentricities, Journal of Constructional Steel Research 2012; 68 (1):107-117.

Table 1. Test properties and results.

Nomenclature	Test	b mm	h mm	t mm	λ	e_{top} mm	e_{bot} mm	f_y MPa	f_c MPa	N_{EXP} kN	N_{EC4} kN	N_{exp}/N_{EC4}
S100.100.4_90.275_20.20	1	100	100	4	0.88	20	20	375.7	88.3	490.7	594.0	0.83
S100.100.4_30.275_20.20	2	100	100	4	0.68	20	20	292.7	36.4	380.8	421.0	0.90
R100.150.4_90.275_20.20	3	150	100	4	0.87	20	20	298.5	86.4	804.3	772.3	1.04
R100.150.4_30.275_20.20	4	150	100	4	0.69	20	20	312.3	30.7	535.8	566.6	0.95
R100.150.5_90.275_20.20	5	150	100	5	0.92	20	20	459.8	83.0	935.0	969.5	0.96
R100.150.5_30.275_20.20	6	150	100	5	0.71	20	20	332.9	32.8	605.6	674.9	0.90
S100.100.4_90.275_50.50	7	100	100	4	0.88	50	50	358.2	91.4	321.1	327.3	0.98
S100.100.4_30.275_50.50	8	100	100	4	0.71	50	50	346.2	35.0	244.0	274.6	0.89
R100.150.5_90.275_50.50	9	150	100	5	0.88	50	50	336.2	92.7	458.5	530.7	0.86
R100.150.4_30.275_50.50	10	150	100	4	0.72	50	50	362.7	31.4	356.0	367.0	0.97
R100.150.5_90.275_50.50	11	150	100	5	0.87	50	50	368.0	84.0	528.1	528.8	1.00
R100.150.5_30.275_50.50	12	150	100	5	0.73	50	50	396.0	26.1	395.0	437.2	0.90
S100.100.4_90.275_20.10	13	100	100	4	0.84	20	10	280.0	93.9	525.7	617.6	0.85
S100.100.4_30.275_20.10	14	100	100	4	0.72	20	10	353.2	37.1	457.3	505.5	0.90
R100.150.4_90.275_20.10	15	150	100	4	0.90	20	10	342.0	90.4	850.9	910.7	0.93
R100.150.4_30.275_20.10	16	150	100	4	0.67	20	10	280.0	31.0	591.7	581.7	1.02
R100.150.5_90.275_20.10	17	150	100	5	0.91	20	10	424.5	86.5	981.6	1047	0.94
R100.150.5_30.275_20.10	18	150	100	5	0.68	20	10	299.2	32.8	654.3	688.8	0.95
S100.100.4_90.275_50.25	19	100	100	4	0.87	50	25	358.6	87.1	383.1	388.7	0.99
S100.100.4_30.275_50.25	20	100	100	4	0.71	50	25	358.6	33.4	253.4	310.2	0.82
R100.150.4_90.275_50.25	21	150	100	4	0.94	50	25	424.5	90.8	463.4	570.9	0.81
R100.150.4_30.275_50.25	22	150	100	4	0.77	50	25	424.5	33.1	311.2	456.7	0.68
R100.150.5_90.275_50.25	23	150	100	5	0.84	50	25	293.5	85.9	526.4	575.2	0.92
R100.150.5_30.275_50.25	24	150	100	5	0.67	50	25	293.5	29.2	391.2	438.0	0.89
S100.100.4_90.275_20.0	25	100	100	4	0.87	20	0	363.2	89.5	652.6	742.5	0.88
S100.100.4_30.275_20.0	26	100	100	4	0.72	20	0	358.2	35.8	474.7	540.6	0.88
R100.150.4_90.275_20.0	27	150	100	4	0.87	20	0	280.0	90.6	926.3	960.4	0.96
R100.150.4_30.275_20.0	28	150	100	4	0.68	20	0	308.4	29.5	624.4	653.4	0.96
R100.150.5_90.275_20.0	29	150	100	5	0.89	20	0	370.3	89.6	1066	1151	0.93
R100.150.5_30.275_20.0	30	150	100	5	0.70	20	0	306.3	36.3	728.5	786.1	0.93
S100.100.4_90.275_20.-10	31	100	100	4	0.87	20	-10	346.9	92.7	737.0	853.5	0.86
S100.100.4_30.275_20.-10	32	100	100	4	0.71	20	-10	346.9	34.1	526.2	542.4	0.97
R100.150.4_90.275_20.-10	33	150	100	4	0.87	20	-10	268.1	93.6	945.8	1107	0.85
R100.150.4_30.275_20.-10	34	150	100	4	0.66	20	-10	268.1	31.7	563.3	626.5	0.90
R100.150.5_90.275_20.-10	35	150	100	5	0.86	20	-10	304.5	93.4	1042	1260	0.83
R100.150.5_30.275_20.-10	36	150	100	5	0.68	20	-10	304.5	30.6	720.2	746.7	0.96
S100.100.4_0.275_20.-10	37	100	100	4	-	20	-10	327.4	0	389.9	**Aver.**	**0.91**
R100.150.4_0.275_20.-10	38	150	100	4	-	20	-10	309.5	0	371.2	**STDev**	**0.07**
R100.150.5_0.275_20.-10	39	150	100	5	-	20	-10	334.6	0	525		
S100.100.4_0.275_50.25	40	100	100	4	-	50	25	327.4	0	238.7		
R100.150.4_0.275_50.25	41	150	100	4	-	50	25	279.6	0	231.7		
R100.150.5_0.275_50.25	42	150	100	5	-	50	25	298.7	0	292		